ACS Sustainable Chemistry & Engineering

pubs.acs.org/journal/ascecg

Research Article

Sustainable Nutrient Substrates for Enhanced Seedling Development in Hydroponics

Zhitong Zhao, Tao Xu, Xiaoyong Pan, Susanti, Jason C. White, Xiao Hu, Yansong Miao, Philip Demokritou, and Kee Woei Ng*

Cite This: *ACS Sustainable Chem. Eng.* 2022, 10, 8506−8516

Read Online

ACCESS | Metrics & More | Article Recommendations | Supporting Information

ABSTRACT: Sustainable agriculture can be achieved by upcycling and repurposing organic wastes for high-value applications. Keratin and cellulose are two natural biopolymers which are plentiful in biowastes such as hair, poultry feathers, wood shavings, and vegetable trimmings. In this study, these waste-derived biopolymers are converted into bioactive nutrient substrates that can support crop development in hydroponic culture systems. Keratin extracted from human hair (HHK) and cellulose nanofibers (CNFs) obtained from wood pulp were fabricated into composite substrates by freeze-drying. The substrates exhibited highly microporous structures, superior hydrophilicity, and excellent mechanical resilience. The obtained substrates not only serve as a physical carrier to support seed germination and seedling development but also function as advanced nutrient delivery platforms by the incorporation and controlled release of micronutrient-doped carbon dots, in addition to keratin degradation. Functional experiments using the model plant Arabidopsis and crops including Bok Choy (*Brassica rapa*) and Arugula (*Eruca vesicaria*) indicated that these substrates have the potential to be customized for enhanced seedling development in comparison to conventional substrates. This study demonstrates the feasibility and potential of upcycling and repurposing keratinous and cellulosic wastes to provide a sustainable solution for targeted nutrient delivery to crops.

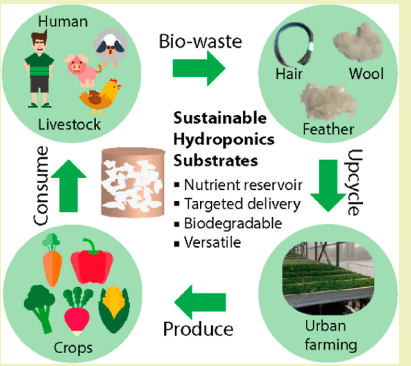

KEYWORDS: *keratin, cellulose, hydroponic substrates, seedling development, sustainable agriculture*

Downloaded via 155.69.170.63 on August 24, 2022 at 02:48:31 (UTC).
See https://pubs.acs.org/sharingguidelines for options on how to legitimately share published articles.

INTRODUCTION

Urban agriculture refers to food production systems inside city boundaries or densely populated areas. In the context of climate change and global industrialization, urban agriculture has drawn increasing interest to achieve global food security.[1] The current COVID-19 pandemic has further driven food insecurity concerns as regional transport of foods has been impeded by pandemic-induced controls, but this has also highlighted one of the biggest advantages of urban agriculture: the ability to produce food locally. Hydroponics is an advanced system in agriculture that has been widely applied in urban farming for soil-less food production. Systems are categorized into two types: solution and medium-culture hydroponics.[2−4] The latter is the dominant type and requires growth media (solid substrates) to support seed germination and crop growth. Currently, hydroponic substrates are largely based on inert materials such as rockwool, expanded clay, perlite, coconut chips, glass wool, and phenolic foam, among others.[3,5,6] However, each of these substrates has its own drawbacks. For example, rockwool is prone to producing small dust particles that could cause human health issues upon inhalation; it is also non-biodegradable and hence not environmentally friendly.[7] Perlite only retains water for a short time and needs to be watered frequently.[3,7] Phenolic foam is not readily biodegradable, resulting in plastic pollution upon disposal.[8] Additionally, the foams may contain toxic constituents that can be released during their lifetime.[4,9] In particular, the abovementioned substrates only serve as inert physical supports for plants and do not deliver nutrients/agrichemicals in a controllable manner to crops, leading to unnecessary pollution and waste in hydroponic systems.[10,11]

Keratin is found abundantly in many epidermal appendages such as hair, wool, horns, hooves, and feathers, many of which are produced in large amounts in agriculture as biowastes.[12−14] Keratin has been extensively explored as a biomedical material for tissue repair, drug release, and wound dressing due to its high biocompatibility and bioactivity.[15−18] However, keratin materials have not been investigated as a substrate in hydroponics to support crop growth in agriculture.[19,20] Since keratin could be extracted from many farm wastes,[21] developing keratin-based hydroponic substrates could be an important strategy for recycling farm wastes as part of sustainable agriculture. In addition, keratin is composed of various amino acids such as

Received: March 21, 2022
Revised: June 3, 2022
Published: June 23, 2022

© 2022 The Authors. Published by American Chemical Society

glycine, alanine, and cysteine with thiol and carboxyl groups,[12,22] which could be exploited to bind cationic micronutrients, thereby functioning as a store for their release under controlled conditions. However, keratin does have poor mechanical properties and low water-swelling capacity that could impede its use as a hydroponic substrate. To mitigate these shortfalls, nanofibrous cellulose could be incorporated into the polymer matrix of keratin. Here, nanocellulose could improve the mechanical properties due to its crystalline domains and the potential for physical cross-links through hydrogen bonds.[23−25] In addition, nanocellulose could enhance the water retention ability of keratin due to the significant number of hydroxyl groups.[26] Additionally, cellulose is a common type of biopolymer with excellent biocompatibility and biodegradability and can be obtained from many farm wastes, such as fruit peels and vegetable trimmings, among others;[27−29] this feature also aligns with the concept of sustainable agriculture. In addition, minimal cytotoxicity of nanocellulose has been revealed by in vitro and in vivo toxicological studies upon ingestion, further ensuring the safety of crops grown with keratin-cellulose materials.[30−32]

Herein, a waste-derived, non-toxic, biodegradable, and sustainable hydroponic substrate was fabricated by combining keratin and cellulose materials. Keratin and cellulose materials were extracted from human hair waste[33−35] and softwood pulp fibers,[36] respectively. Freeze-drying was employed as a convenient synthesis method to fabricate keratin-cellulose composite substrates. During freezing, the system consists of nucleating ice crystals dispersed among non-frozen liquid microphase compartments in which the biomolecules present are highly concentrated but mobile. This forces the biomolecules closer to one another to engage in intermolecular interactions, thereby contributing to the structure of the eventual substrates.[34] Ice crystals serve as porogens, resulting in the formation of interconnected pores after sublimation. The resultant hydroponic substrates have high porosity and interconnectivity of pores, and good mechanical properties with high resilience under aqueous conditions. In addition, this keratin-based substrate could absorb and retain large quantities of water as a promising growth medium to support seed germination and crop growth in hydroponics. To evaluate whether the keratin-cellulose substrate can also be used as a smart delivery platform of agrichemicals, carbon dots (CDs) were incorporated into the polymer matrix. CD is one type of carbon-based nanomaterial and has been proven to enhance crop growth by enhancing photosynthesis.[37−39] In addition, copper, as an essential plant micronutrient,[40,41] is doped into CDs (CuCDs) prior to being supplemented into the substrates.[10,42] Seeds of *Arabidopsis*, *Bok Choy*, and *Arugula* were cultured on the substrates, followed by evaluating the seedling development via measuring root/shoot elongation and biomass. In this study, the novel keratin/cellulose-based hydroponic substrate could overcome the challenges faced by other growth media associated with sample handling, waste disposal, environmental protection, and risk to human health and may be a novel sustainable substrate for hydroponics and urban agriculture applications.

MATERIALS AND METHODS

Materials. Ethanol, thiourea, citric acid, ethylenediaminetetraacetic acid (EDTA), and $CuCl_2$ (≥99%) were acquired from Sigma-Aldrich. Methanol and SnakeSkin dialysis tubing (10K MWCO) were acquired from Thermo Fisher Scientific. Urea (99.5−100.5% Chem-Impex) and 1,4-dithio-DL-threitol (DTT, ≥ 99%) were acquired from Chem-Impex. Softwood-bleached Kraft fiber was acquired from St. Felicien Mill, Canada.

Extraction of Human Hair Keratin (HHK). A "two-step" reductive method was used to extract keratin from human hair waste as described in our previous work.[34,35] Briefly, the hair fragments were incubated in 25 mM Tris−HCl (pH 9.5) buffer solution consisting of 25% v/v ethanol, 200 mM DTT, and 8 M urea for 72 h at 50 °C to remove keratin-associated proteins (KAPs). Then, keratin was extracted from the KAP-free hair by incubation in another Tris−HCl (pH 8.5) solution containing 200 mM DTT, 5 M urea, and 2.6 M thiourea for 24 h at 50 °C. Finally, the extraction was filtered and dialyzed against deionized (DI) water using SnakeSkin dialysis tubing (10K MWCO). The content of keratin in solution was determined by dry weight determination before use.

Preparation of Cellulose Nanofibers (CNFs). The mechanical grinding method was used to prepare CNFs as described in the literature.[27,43] Soft wood fiber was ground by an ultra-fine friction grinder manufactured by Masuko Sangyo Co (Kawaguchi, Japan). The obtained CNF has a size of approximately 50 nm, and we prepared a stock solution of CNF that was 2% w/w in water.

Preparation of Carbon Dots and Copper-Doped Carbon Dots. Briefly, 0.6 g of EDTA was dissolved in 50 mL of DI water. The solution was transferred into a 100 mL Teflon-lined steel autoclave. After heating at 200 °C for 10 h, the obtained CD solution, at 11 mg/mL in a 50 mL stock solution, was allowed to cool down to room temperature, followed by centrifugation at 10,000 rpm for 10 min. The precipitate was discarded, and the pH of the supernatant was measured and adjusted to 6.5−7.0. The synthesis of CuCD went through the same protocol, with the addition of 0.2 g of $CuCl_2$ being mixed with EDTA solution before autoclaving.

Fabrication of HHK-CNF Hydroponic Substrates. A previously published freeze-drying protocol was used to fabricate HHK-CNF substrates.[15] Briefly, the keratin solution was mixed with the cellulose solution at different weight ratios (1.5:0.25, 1.5:0.5, and 1.5:0.75 wt %) prior to being poured into a 24-well culture plate, and the mixture solution was then frozen at −20 °C for overnight. To incorporate the agrichemicals, CD and CuCD were added to the keratin-cellulose mixture solution before freezing. A CuCD stock solution (10 mg/mL) was added to obtain the low (0.1 mg/mL) and high (0.5 mg/mL) concentrations of CuCDs in the composite, and the resultant substrates are denoted as HHK-CNF-CuCD-1 and HHK-CNF-CuCD-2, respectively. The frozen samples were sublimed in a freeze-drier for 48 h at −50 °C under 0.1 mbar pressure.

Morphology of Substrates under a Scanning Electron Microscope (SEM). The substrate morphology was observed using a field-emission scanning electron microscope (FESEM, JEOL, JSM-6340F) at an acceleration voltage of 5 keV after sample cross-sections were coated with gold by sputtering at 20 mA for 45 s.

Compression Test on HHK-CNF Substrates. The compression strength of the substrates was measured using an Instron mechanical tester 5567 with a 500 N sensor (Instron Co., Norwood, MA, USA). The samples used for measurement were ∼10 mm thick and ∼15 mm in diameter. The loading speed was set at 1 mm/min, and the strain level was up to 80% of the original height. The compressive moduli were the approximate linear fitting values of the stress−strain curves at the strain of 10%. Each sample has three duplicates to get the average strength.

Porosity of Substrates. To characterize micro-porosity, a liquid displacement method was used as described in the literature.[44] Cylindrical keratin-based substrates (n = 3) were fabricated, and the dimensions were measured using a digital vernier caliper to calculate scaffold volumes (V_s). The dry weight (W_d) of each sample was measured using an electronic analytical balance. The samples were immersed in 20 mL of isopropanol with a density (ρi) of 0.785 g/mL under vacuum overnight to fill pores with isopropanol. The saturated sample was weighed (Ws), and the porosity was calculated using the following eq 1

$$\text{Porosity} = \frac{(w_s - w_d)/\rho_i}{V_s} \times 100\% \quad (1)$$

https://doi.org/10.1021/acssuschemeng.2c01668
ACS Sustainable Chem. Eng. 2022, 10, 8506−8516

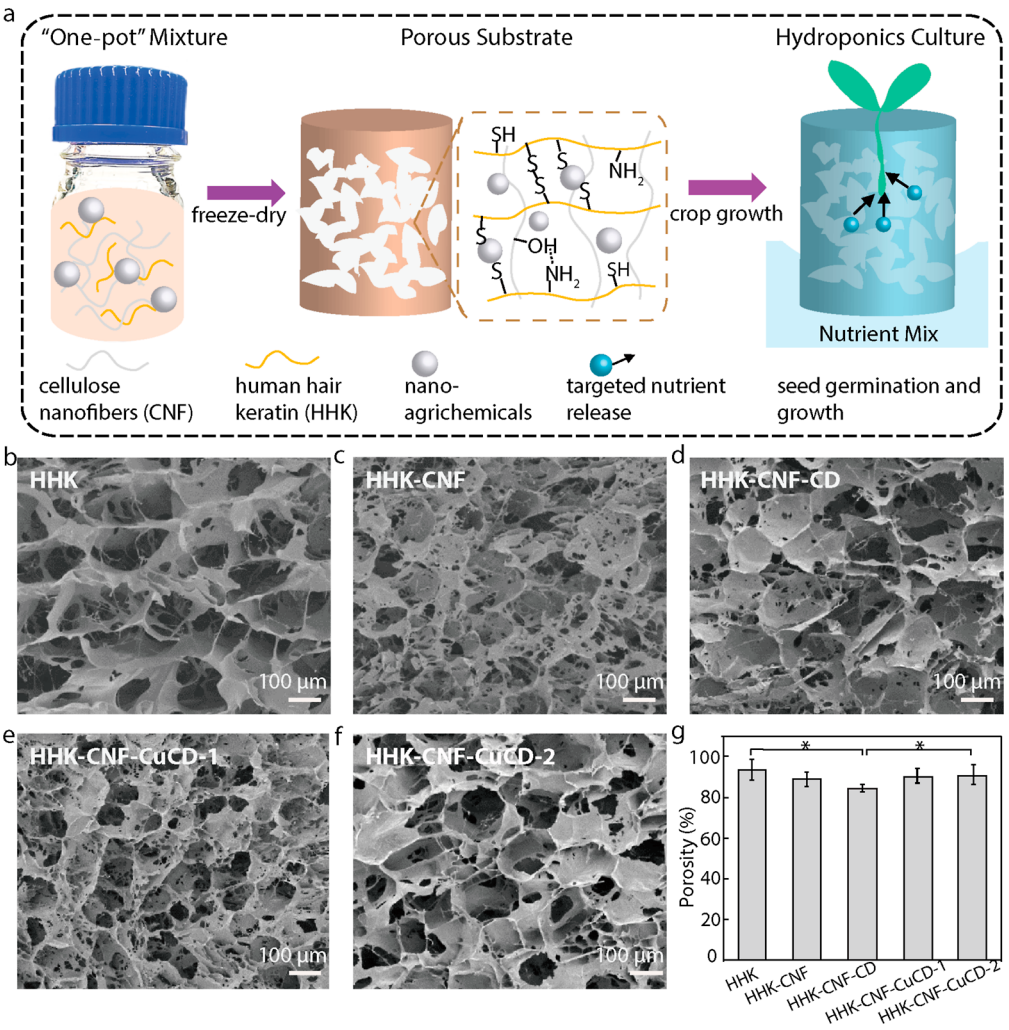

Figure 1. (a) Schematic illustration of the fabrication process of HHK-CNF-agrichemical substrates via a freeze-drying method and their potential use in hydroponics. Morphologies of HHK (b), HHK-CNF (c), HHK-CNF-CD (d), HHK-CNF-CuCD-1 (e), and HHK-CNF-CuCD-2 (f) under SEM. The porosity of all these samples was calculated using a liquid displacement test (g), $*p < 0.05$ (n=3).

Characterization of Water Uptake and Stability of Hydroponic Substrates in Water. The substrates were immersed in water at room temperature for 72 h to reach swelling equilibrium. The samples were weighed (M_{wet}) after removing excess water from their surfaces by gentle blotting. The dry masses of samples (M_{dry}) were measured after rinsing in deionized water and freeze-drying. The water uptake ratio (S) was calculated using eq 2

$$S = \frac{M_{wet} - M_{dry}}{M_{dry}} \quad (2)$$

To evaluate the stability of substrates under aqueous conditions, the mass loss of samples was determined after 1 week of incubation in water. The weights of the remaining samples were measured after drying and compared to their original weights. All samples were measured in triplicate.

Additionally, the mechanical integrity of substrates under hydroponic conditions was also determined. After 72 h of immersion in water, all samples were subjected to the compression test using the Instron mechanical tester 5567 (Instron Co. MA, USA) as described above. To evaluate the robustness of samples, the swollen samples were also subjected to loading−unloading of the compression force for several cycles.

Cu^{2+} Ions and Keratin Release Profiles. Cu^{2+} ions released from CuCDs within the keratin-based substrates were measured using inductively coupled plasma spectrometry-optical emission spectrophotometers (ICP-OES, Horiba, Japan). The samples were immersed in 10.0 mL of DI water at room temperature, and the medium was collected at predetermined time points (1, 3, and 8 h on 1, 2, 3, 5, 7, and 14 days) for Cu^{2+} release kinetics determination. The concentration of soluble keratin in the medium was determined with a MicroBCA assay. All samples have triplicates to calculate an average value.

Plant Growth Test. Bok Choy and Arugula seeds were purchased from a local store and sown on the keratin-based substrates within DI water as displayed in Figure 8a. Plant growth experiments were performed in a hood (50% relative humidity) at RT ~22 °C with 14 h of light culture and 10 h of dark culture, randomly designed with two replications and six seeds for each replicate. The samples were watered every 2 days. The seedlings were harvested, and the root length, shoot length, and fresh weight of seedlings (roots excluded) were evaluated after 10 days of growth. *Arabidopsis thaliana* seeds were also grown in HHK-based substrates following the same protocol but with 30−40 seeds cultured on each substrate.

Statistical Analysis. The statistical analysis of the water-swelling ratios of the substrates, mechanical properties, and seedling development was carried out with a one-way ANOVA using SPSS version 20.0, followed by Tukey's post-hoc analysis. Comparisons of the means between two groups were carried out with Student's *t*-test.

RESULTS AND DISCUSSION

The fabrication process of keratin-cellulose substrates using a freeze-drying method is illustrated in Figure 1a. The keratin

https://doi.org/10.1021/acssuschemeng.2c01668
ACS Sustainable Chem. Eng. 2022, 10, 8506−8516

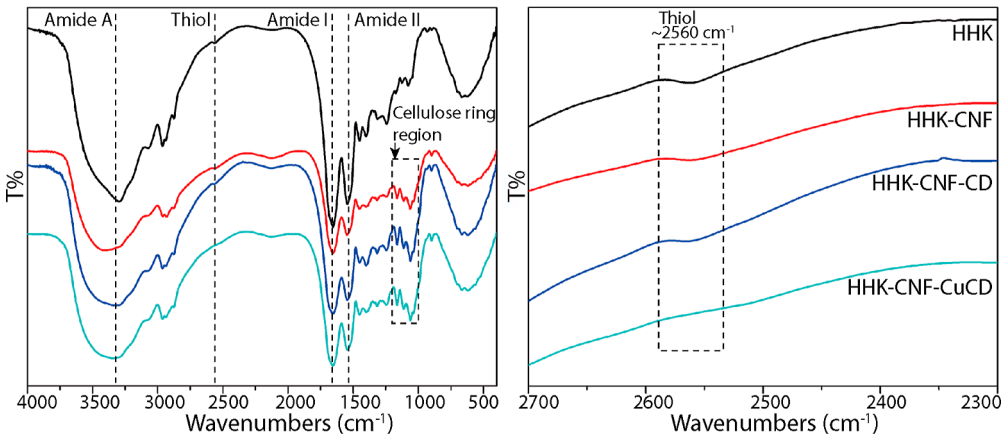

Figure 2. Fourier transform infrared spectroscopy (FTIR) spectra of HHK, HHK-CNF, HHK-CNF-CD, and HHK-CNF-CuCD samples.

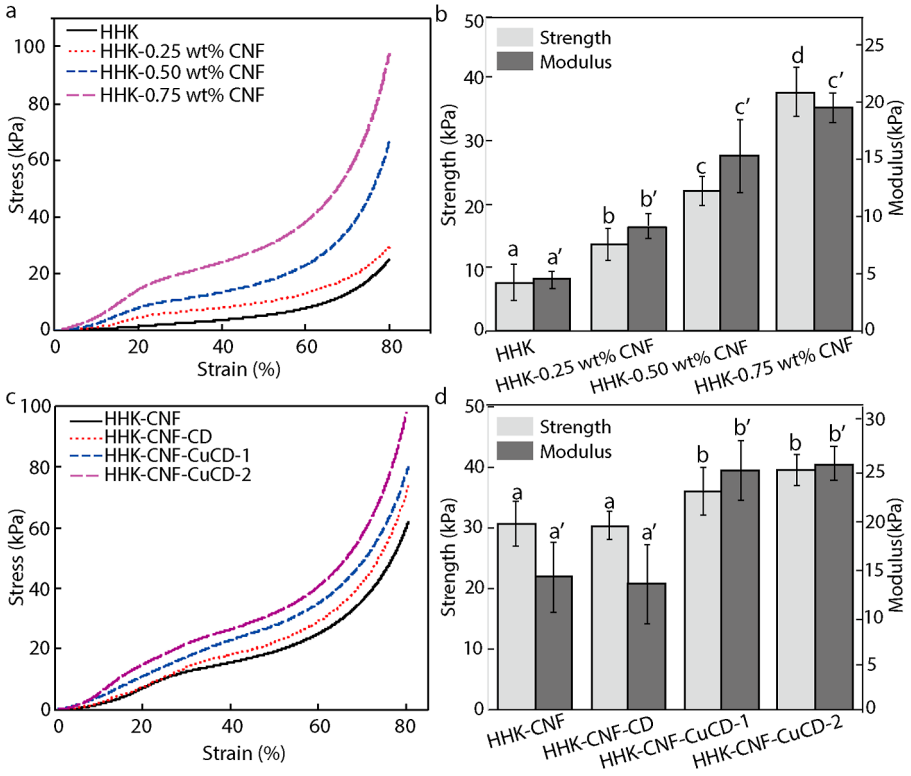

Figure 3. Compressive properties of hydroponic substrates. (a,c) Representative stress−strain curves of keratin-based substrates with varying CNF weight contents and HHK-CNF substrates containing CD and CuCD agrichemicals, respectively. HHK-0.5 wt % CNF was used as the matrix to incorporate agrichemicals. (b,d) Plots of average compressive strength at 60% strain and elastic modulus across substrates with different weight contents of CNFs and substrates containing different agrichemicals. Samples marked by different letters are significantly different from one another, while those marked by the same letter are not significantly different ($p < 0.05$, $n = 3$; one-way ANOVA followed by Tukey's post-hoc analysis).

materials were mixed with CNFs (~50 nm in diameter) in a "one-pot" followed by adding CD and CuCD solutions as nano-agrichemicals. The mixture was stirred vigorously prior to being cast into plastic molds and frozen at −20 °C overnight. In the freezing process, keratin and cellulose are condensed around the growing ice crystals, leading to the close proximity of the molecules. This significantly encourages cross-linking, primarily through disulfide linkages between keratin and secondary hydrogen bonding to form interconnected composite networks.[35] Upon lyophilization to remove the ice crystals, an agrichemical-enriched keratin-cellulose porous substrate was obtained. During the fabrication, water was the only solvent used to dissolve all components, highlighting the relative simplicity of this fabrication strategy. Theoretically, the resultant keratin-cellulose-based substrates could be fabricated into various shapes and sizes by varying the morphology of the mold.

The microstructure of substrates was investigated under SEM and is shown in Figure 1b−f. All substrates exhibited a well-interconnected network of pores, with the pore size range being approximately ~100 to ~200 μm. The high interconnectivity revealed by SEM suggests that these substrates could be conducive to water and nutrient delivery to plant roots during hydroponic growth. It is also worth noting that the pores seemed to be well-formed in the samples that contained CuCDs, without displaying defects on the polymeric walls of the pores (Figure 1f). This could be due to the formation of metal-thiolate

https://doi.org/10.1021/acssuschemeng.2c01668
ACS Sustainable Chem. Eng. 2022, 10, 8506−8516

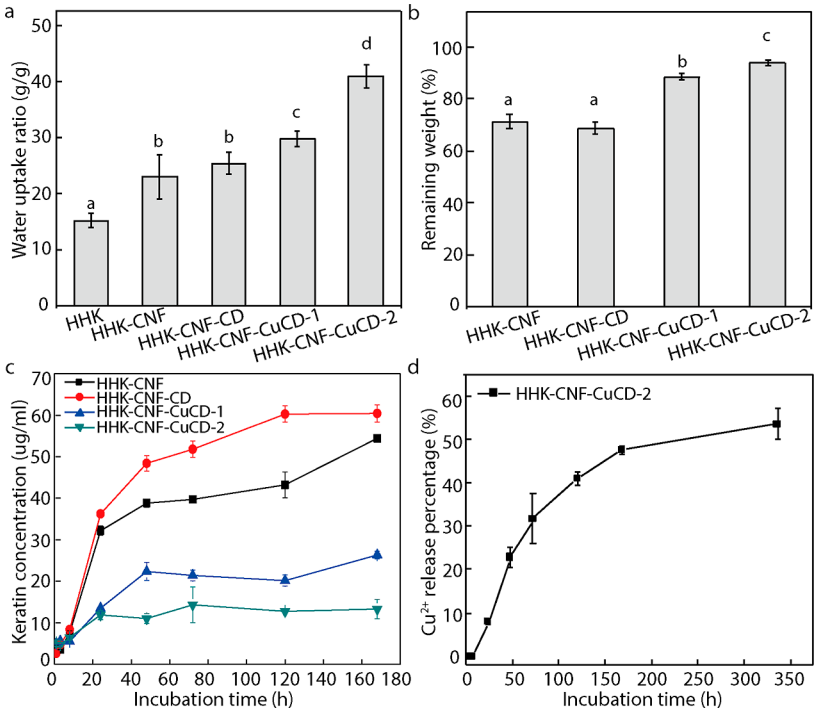

Figure 4. Stability of keratin-cellulose substrates under aqueous conditions. (a) Water uptake ratio of the substrates after 72 h of incubation in DI water at room temperature. (b) Remaining weights of the substrates after 1 week of immersion in water. (c) Profile of released keratin from the substrates in water (n=3). (d) Cu^{2+} release kinetics of HHK-CNF-CuCD-2 in 2 weeks in DI water (n=3). Samples marked by different letters are significantly different from one another, while those marked by the same letter are not significantly different ($p < 0.05$, n=3; one-way ANOVA followed by Tukey's post-hoc analysis).

complexes, resulting in a further highly cross-linked network formed between Cu^{2+} ions in CuCDs and thiol groups in keratin.[45] The combination of thiol groups of keratin and cationic nutrients could make the keratin-cellulose substrates a platform for the controlled release of nutrients/agrichemicals in hydroponics, as illustrated in Figure 1a. Porosities of all substrates were determined with a liquid replacement test. As shown in Figure 1g, all substrates displayed high porosities above ~90%, which is beneficial for both water retention and the exchange of gases/nutrients from the substrates to the surroundings.

To understand the potential interactions among HHK, CNFs, and CDs/CuCDs, we analyzed FTIR spectra of the substrates. As shown in Figure 2, the spectra of all substrates exhibit characteristic bands of their respective components. The 3280 cm^{-1} band can be assigned to N−H stretch vibration of amide A in keratin. The characteristic peaks at 1700−1600 and 1550 cm^{-1} are due to the C═O (amide I of keratin) stretch and C−N stretch (amide II) vibrations of keratin, respectively.[46,47] In particular, a weak band is centered at ~2560 cm^{-1} in the spectrum of HHK, HHK-CNFs, and HHK-CNF-CDs, which can be attributed to the free thiol groups of keratin.[22,35] However, this weak band is absent in the spectra of HHK-CNF-CuCD samples, suggesting that the chemical reactions might have occurred between thiols of HHK and CuCDs. According to the literature, Cu^{2+} ions of CuCD could combine with thiol groups to form metal-thiolate coordinate bonds.[45,48] It should also be noted that the non-frozen liquid microphase, which becomes highly concentrated with HHK, CNFs, and nano-agrichemicals due to the freezing process, further facilitates these chemical reactions.[34] The bands between 1200 and 900 cm^{-1} could be due to sugar ring deformations of cellulose.[47] Overall, the simple mixture of keratin, cellulose, and agrichemicals did not markedly alter the chemical structures of each individual component. The combination between thiol groups of keratin and Cu^{2+} ions of CuCDs further highlights that this keratin-cellulose-based substrate might be used as the platform that could control the release of cationic micronutrients in a hydroponic culture system.

Compressive tests were performed to assess whether CNFs enhanced the mechanical properties of the keratin-cellulose substrates. The samples were fabricated into cylindrical shapes with a diameter of ~15 mm and a thickness of ~10 mm for the tests. As evident from the stress−strain curves shown in Figure 3a, all samples were compressed under an increasing strain without displaying a break point. The compressive strength calculated at 60% strain in Figure 3b exhibited a significant increase with increasing weight content of CNF, revealing the significant reinforcement effect of CNFs. The substrates containing 0.75 wt % CNFs recorded a strength of ~40 kPa, which was ~four times greater than that of the HHK-only substrate (~10 kPa). Meanwhile, the compressive modulus was increased to ~18.7 kPa, which was ~six times that of the HHK-only sample (~3.9 kPa). As expected, the increase in compression strength and stiffness can be attributed to the dense networks of CNF formed within the keratin matrix via hydrogen bonds.

The CDs and CuCDs were incorporated into the keratin-cellulose substrates that contained 0.5 wt % CNFs to investigate the effect of nano-agrichemicals on mechanical properties. As shown in Figure 3c,d, the strength of substrates increased from ~30 to ~40 kPa once CuCD was incorporated into the keratin-cellulose matrix. Meanwhile, the moduli of HHK-CNF-CuCDs increased from ~14 to ~27 kPa in comparison with HHK-CNF

https://doi.org/10.1021/acssuschemeng.2c01668
ACS Sustainable Chem. Eng. 2022, 10, 8506−8516

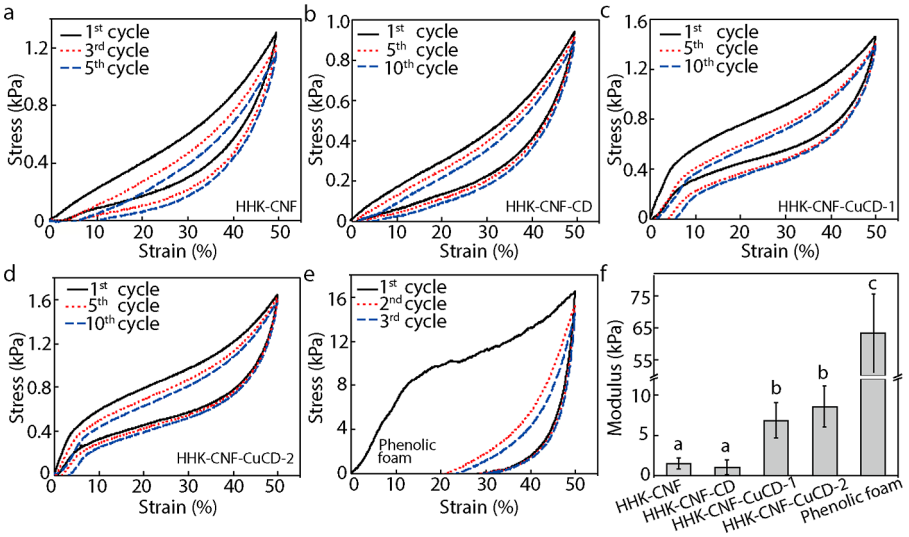

Figure 5. Comparison of the mechanical resilience of keratin-cellulose substrates under hydroponic conditions. (a–e) Representative stress–strain curves of HHK-CNF (a), HHK-CNF-CD (b), HHK-CNF-CuCD-1 (c), HHK-CNF-CuCD-2 (d), and phenolic foams (e) over different cycles of loading and unloading at 50% strain. The maximum stresses recorded are ~1.3, ~0.9, ~1.5, ~1.6, and ~15.6 kPa, respectively. Mean compressive moduli were calculated and plotted in (f). Samples marked by different letters are significantly different from one another, while those marked by the same letter are not significantly different ($p < 0.05$, $n = 3$; one-way ANOVA followed by Tukey's post-hoc analysis).

samples. This result demonstrates that the incorporation of CuCDs enhanced the mechanical properties of the resultant substrates owing to the cross-linked networks formed between Cu^{2+} ions of CuCD and thiol groups of keratin. Overall, the superior mechanical properties indicate that the keratin/cellulose-based substrates are adequate to withstand routine handling, which is crucial for agricultural applications. The content of CNF in the keratin-based substrates for the following tests was subsequently fixed at 0.5 wt % during sample fabrication.

Another important property of hydroponic substrates is their ability to retain sufficient water to support crop growth, which can be evaluated by water uptake capacity. Thus, various substrates were immersed in deionized water at room temperature for 72 h for evaluation. As shown in Figure 4a, the overall water uptake ratio of HHK-CNF substrates was significantly higher than that of HHK samples; this can be attributed to the presence of CNFs with significant quantities of −OH groups. Notably, the incorporation of CuCDs further enhanced the water absorption ability of HHK-CNF substrates with a significant increase in the water uptake ratio. As the content of CuCDs increased, HHK-CNF-CuCD samples could absorb water at ~40 times their weight, which is comparable to that of commercial phenolic foam in hydroponics. The enhanced water retention ability can be attributed to the cross-linked polymer networks formed between thiol groups of keratin and Cu^{2+} ions of CuCDs. The high water-swelling capacity could aid in maintaining a balance between absorption of the nutrient solution and simultaneously not dehydrating plants in hydroponics.

The degradation property of the keratin-cellulose substrates was also assessed under aqueous conditions. Ideally, the degradation rate of hydroponic substrates should correlate with the growth period of the intended crop, which could range from a few weeks to a few months. In this study, the degradation of substrates was examined for only 1 week to reveal preliminary trends. After 1 week of incubation in water, HHK-CNF-CuCD samples lost less than 10% of the original mass, compared to ~25% mass loss for HHK-CNFs and HHK-CNF-CD samples (Figure 4b). This suggests that Cu^{2+}-thiol cross-linking could enhance the stability of the substrates in water. The degradation rate of various substrates was also profiled by the released keratin in the water. As shown in Figure 4c, all substrates had a burst release of keratin within the first 24 h, but the released concentration of keratin for HHK-CNF-CuCDs (~10 μg/mL) is much lower than that of samples without CuCDs (~35 μg/mL). The release of keratin then reached an equilibrium for the substrates containing CuCDs within 2 days, but the other substrates continued to release keratin until 5 days of incubation. Collectively, these findings indicate that the keratin-cellulose substrates can be a source of carbon and nitrogen for plants through keratin degradation. Cross-linking between the Cu^{2+} ions of CuCD and the thiol of keratin enhanced the structural integrity of substrates under aqueous conditions, which should enhance substrate stability during the period of crop growth.

To evaluate the potential of keratin-cellulose substrates as the platform for micronutrient release, Cu^{2+} release kinetics were assessed by ICP-OES for the samples containing a high content of CuCDs. Figure 4d summarizes the Cu^{2+} release kinetics over time for HHK-CNF-CuCD-2 in DI water. The release profile showed an obvious Cu^{2+} release within the first 72 h. Then, the system reached an equilibrium at approximately 55% release of Cu^{2+} at 2 weeks. It is worth noting that different types of crops may require different amounts of micronutrients during germination and seedling development. Therefore, it is important to develop keratin-cellulose hydroponic substrates with tunable agrichemical release kinetics; synthesis could involve modulating the keratin-cellulose composition and the molar ratio between keratin and micronutrients in the substrates. In the future, long-term degradation and nutrient release tests will be performed in the field under various hydroponic conditions.

The structural resilience of hydroponic substrates under aqueous conditions is important not only for routine handling but also for physical support of seedlings. Thus, the mechanical integrity of keratin-cellulose substrates was determined by

https://doi.org/10.1021/acssuschemeng.2c01668
ACS Sustainable Chem. Eng. 2022, 10, 8506−8516

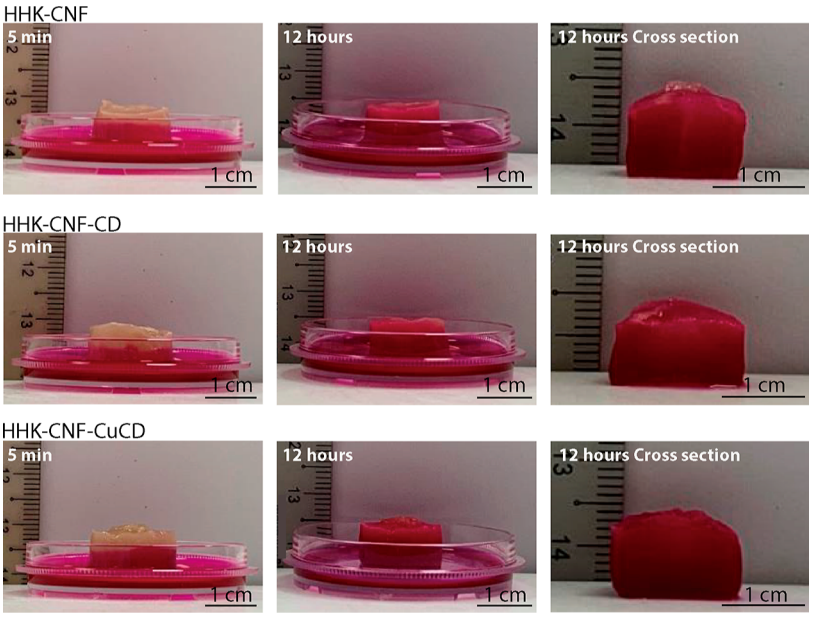

Figure 6. Water/nutrient absorption and distribution behavior within various keratin-cellulose substrates. Rhodamine (red) was incorporated for visualization.

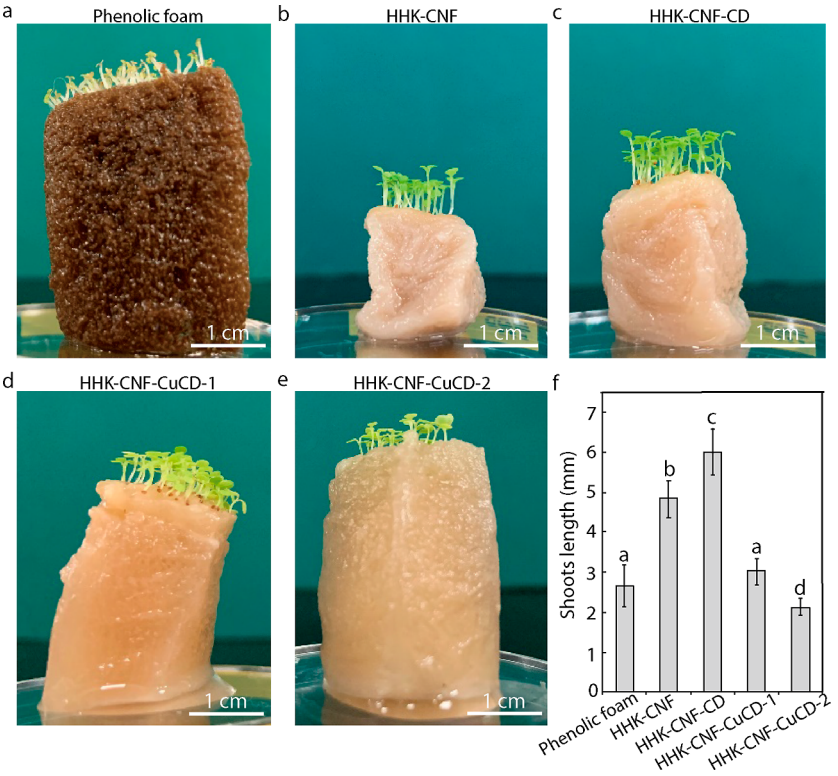

Figure 7. (a–e) Photographs of Arabidopsis seedlings on phenolic foam (a), HHK-CNF (b), HHK-CNF-CD (c), HHK-CNF-CuCD-1 (d), HHK-CNF-CuCD-2 (e), and their shoot lengths after 10 days (f). Samples marked by different letters are significantly different from one another, while those marked by the same letter are not significantly different ($p < 0.05$; one-way ANOVA followed by Tukey's post-hoc analysis).

performing cyclic compressive tests on water-swollen samples. As the stress–strain curves show in Figure 5, the strength of HHK-CNF substrates at 50% strain increased from ~1.3 kPa (Figure 5a) to ~1.6 kPa upon CuCD incorporation (Figure 5d). As demonstrated by the elastic moduli calculated in Figure 5f, HHK-CNF-CuCD substrates have a greater stiffness value of ~7.5 kPa compared to that of HHK-CNF (~1.6 kPa) and HHK-CNF-CD substrates (~1.2 kPa), respectively. These results indicate that the cross-linking between Cu^{2+} ions of CuCDs and thiol groups of keratin enhanced the mechanical integrity of the substrates under aqueous conditions as well. It is noteworthy that the compressive properties of all substrates decreased significantly once immersed in water in comparison to those of dry samples, as shown in Figure 3. This could be attributed to the absorbed water disrupting hydrogen bonds, leading to more flexible polymer networks. During crop growth, mechanical

https://doi.org/10.1021/acssuschemeng.2c01668
ACS Sustainable Chem. Eng. 2022, 10, 8506–8516

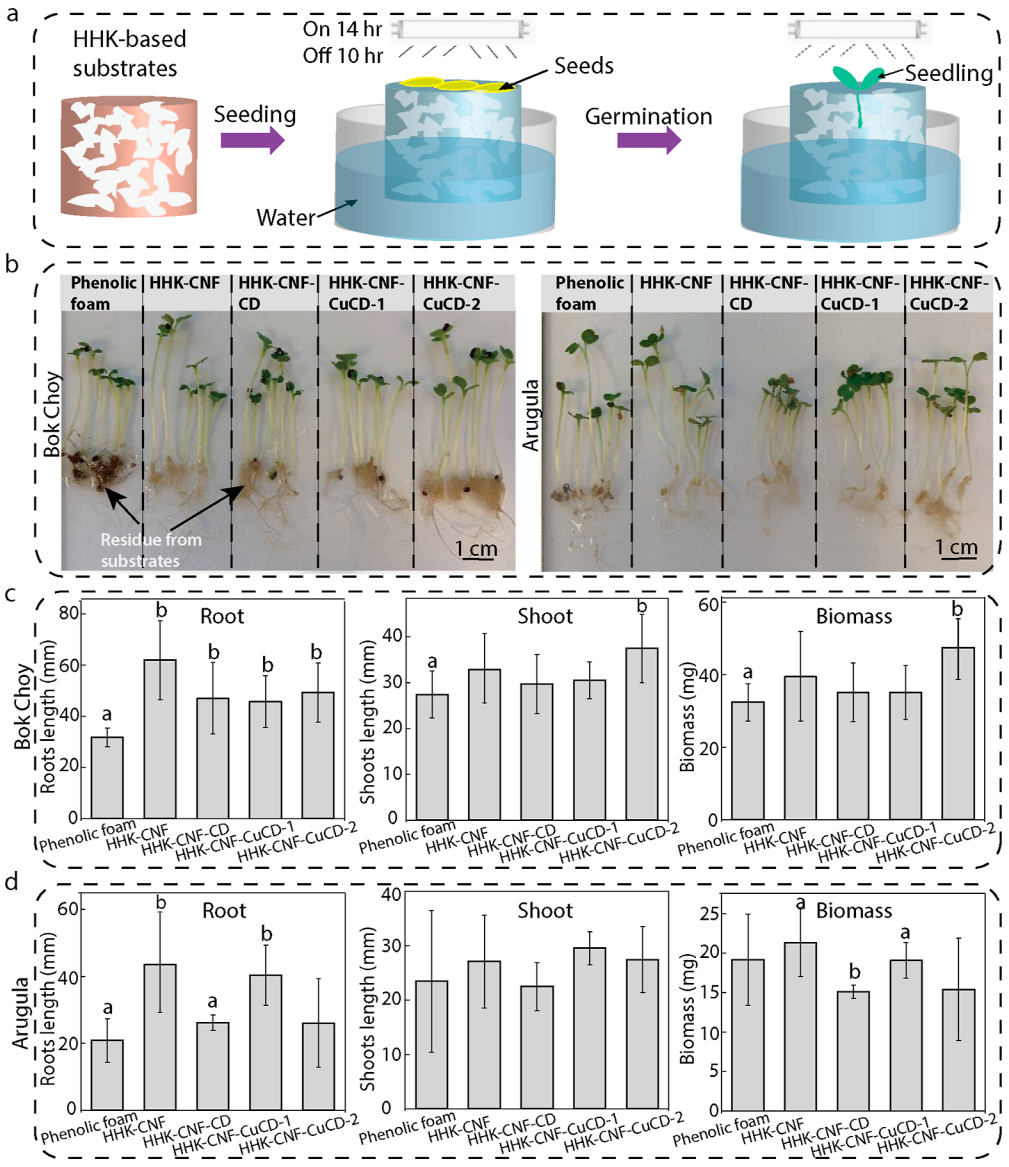

Figure 8. Schematic illustration of the plant growth experiment on various keratin-cellulose hydroponic substrates (a). (b) Photographs of Bok Choy and Arugula seedlings after 10 days of growth. Comparison of root and shoot lengths and the fresh weight of seedlings (biomass) in HHK-CNF, HHK-CNF-CD, HHK-CNFCuCD-1, and HHK-CNF-CuCD-2 for Bok Choy (c) and Arugula (d). Samples marked by different letters are significantly different from one another, while those marked by the same letter are not significantly different ($p < 0.05$, n=6; one-way ANOVA followed by Tukey's post-hoc analysis).

resilience is also crucial because the seedlings in the substrates require routine handling such as transplantation or transportation. To evaluate this, water-swollen samples were subjected to cyclic compressive tests at a maximum strain of 50% as shown in Figure 5a–e. HHK-CNF-CuCD-2 shows a maximum compressive stress of ~1.6 kPa with 50% strain, and the sample still retains this maximum stress after 10 cycles of loading–unloading (Figure 5e). Conversely, the maximum stress of HHK-CNFs at 50% strain decreased from ~1.3 to ~1.0 kPa after only five cycles of loading–unloading (Figure 5a). Additionally, the shape recovery of HHK-CNF substrates was enhanced by the incorporation of CuCDs (Supporting Information, Figure S1 and Supplementary Video S1). As shown after five cycles of loading–unloading, ~98% of the shape was recovered for HHK-CNF-CuCD-2, but only ~90% was recovered for HHK-CNF after the stress. These results indicate that the incorporation of CuCDs enhanced the mechanical integrity and resilience of the keratin-cellulose substrates again due to the cross-linking between Cu^{2+} ions of CuCDs and thiol of keratin. The resilience of commercial phenolic foams was also assessed in Figure 5f. As expected, the strength of the phenolic foam was significantly decreased after only three cycles of loading–unloading, and only ~70% of the original shape was recovered (Supporting Information, Figure S1 and Supplementary Video S2). The loss in mechanical integrity could cause dramatic changes in the microstructures of samples, including porosity and pore size, which would lead to low nutrient/gas exchange efficiency within the substrates. Overall, the superior mechanical integrity and resilience of keratin-cellulose substrates could withstand the external mechanical stresses from routine handling in hydroponics, thereby retaining the necessary growth microenvironment for optimal crop growth.

As shown in the SEM images, all keratin-cellulose hydroponic substrates have high porous interconnectivity. To determine

https://doi.org/10.1021/acssuschemeng.2c01668
ACS Sustainable Chem. Eng. 2022, 10, 8506–8516

whether this high interconnectivity can efficiently support nutrient transport within the substrates, an aqueous solution of rhodamine dye was introduced to simulate a mixture of small-molecule nutrients. Three types of keratin-cellulose substrates were evaluated. Optical images were taken at 5 min and 12 h, and results are presented in Figure 6. As the cross-section of samples exhibited, rhodamine dyes can be distributed uniformly within the substrates after 12 h of absorption, suggesting that the large microporous network could provide adequate space for the nutrients to effectively reach plant roots within the substrates. In addition, the excellent wettability of CNFs could promote nutrient absorption into the keratin-cellulose substrates.[26]

To evaluate the potential of keratin-cellulose substrates to support seed germination and seedling growth in hydroponics, *A. thaliana* was cultured on several types of substrates as the first model plant. Although *Arabidopsis* is not a food crop, the test could guide further studies with edible species. A commercial hydroponic substrate based on phenolic foam was employed as the control. Seedling development on various substrates was evaluated by measuring shoot length after 10 days of growth in water without additional nutrients. As shown in Figure 7a−e, all types of substrates can support *Arabidopsis* growth with well-developed seedlings. In comparison to phenolic foams, *Arabidopsis* seedlings on keratin-cellulose substrates developed greener and larger leaves after 10 days. Shoot lengths (Figure 7f) show a significant increase in HHK-CNF and HHK-CNF-CD samples in comparison with phenolic foam. Interestingly, HHK-CNF-CuCD attenuated the positive effects of other keratin-cellulose substrates, with plants having shorter shoots than seedlings on HHK-CNFs and HHK-CNF-CDs. This adverse effect of CuCDs on *Arabidopsis* growth suggests that the plants might require different compositions of cationic micronutrients for their growth. The preliminary plant growth result demonstrates that keratin-cellulose substrates have significant potential for effectively supporting crop growth in hydroponics.

In addition, two edible crops were tested on keratin-cellulose substrates: Bok Choy and Arugula. The root and shoot lengths and biomass of fresh seedlings were measured after 10 days of growth and are shown in Figure 8. Arugula and Bok Choy seedlings developed well on keratin-based substrates, with robust root and shoot systems. It should be noted that Bok Choy on keratin-based substrates developed much longer root systems than those of seedlings on phenolic foam (Figure 8b). As calculated, the root length of Bok Choy increased by ∼103, ∼49, ∼48, and ∼50% upon growing in HHK-CNF, HHK-CNF-CD, HHK-CNF-CuCD-1, and HHK-CNF-CuCD-2 substrates, respectively. This indicates that the roots of Bok Choy were able to penetrate keratin-based substrates (Supporting Information, Figure S2), very effectively absorbing the nutrients released from the substrates into the water.

In contrast, the roots of Bok Choy did not grow well within the phenolic foam, which could be attributed to the high stiffness as calculated in Figure 5. The Bok Choy seedlings on HHK-CNF-CuCD-2 substrates also displayed longer shoots (∼37.2 mm of length) and a greater fresh weight (∼46.7 mg of biomass) compared with those growing on phenolic foam with ∼27.8 mm of length and ∼32.4 mg of biomass. This result indicates that the incorporation of CuCD agrichemical enhanced the seedling development of Bok Choy. As shown in Figure 8d, there is no significant difference among all Arugula groups in terms of the length of shoot and biomass, suggesting that keratin-based substrates could support Arugula growth as well as phenolic foam. These data with edible crops demonstrate that keratin-based substrates can support and improve seedling growth. It is worth noting that different types of crops might require different macronutrient and micronutrient treatment regimens for seedling development. Therefore, it is necessary to develop various platforms of keratin-based substrates that combine different nutrients that may be released at different rates to stimulate crop growth.

CONCLUSIONS

In the present study, keratin and cellulose materials were converted into hydroponic substrates for use as a platform in sustainable agriculture. The keratin-cellulose substrates were fabricated using a facile synthesis method with water as the only solvent. The resultant substrates exhibited a robust microporous structure with high interconnectivity that provides large spaces for nutrient transport. In addition to being a physical carrier for supporting crop growth, the keratin-cellulose substrates also demonstrated potential as a smart platform to control the release of macronutrients through keratin degradation and also the release of cationic micronutrients through the formation of chemical bonds between cationic ions and active thiol groups of keratin during synthesis. Plant growth experiments confirmed that the keratin-cellulose substrates can promote greater seedling development compared to conventional commercial hydroponic substrates. Overall, this proof-of-concept study can valorize biowastes and create a sustainable agriculture model since keratin and cellulose materials can be readily obtained from keratinous materials such as hair and poultry feathers and cellulosic wastes such as fruit peels and vegetable trimmings. In the future, field tests will be performed to evaluate these substrates under more realistic hydroponic culture conditions and to customize substrates to meet the requirements of specific crop types.

ASSOCIATED CONTENT

Supporting Information

The Supporting Information is available free of charge at https://pubs.acs.org/doi/10.1021/acssuschemeng.2c01668.

Bok Choy seedlings grown in the substrates after 10 days (PDF)

Demonstration of the mechanical resilience of HHK-CNF-CuCD substrates when subjected to cycling compression. (MP4) and

demonstration of the lack of mechanical resilience of phenolic foams when subjected to cycling compression (MP4)

AUTHOR INFORMATION

Corresponding Author

Kee Woei Ng − *School of Materials Science and Engineering, Nanyang Technological University, Singapore 639798, Singapore; Center for Nanotechnology and Nanotoxicology, Harvard T.H. Chan School of Public Health, Harvard University, Boston, Massachusetts 02115, United States; Environmental Chemistry and Materials Centre, Nanyang Environment and Water Research Institute, Nanyang Technological University, 637141, Singapore; Singapore-HUJ Alliance for Research and Enterprise (SHARE), Singapore 138602, Singapore;* orcid.org/0000-0002-7276-3563; Email: kwng@ntu.edu.sg

https://doi.org/10.1021/acssuschemeng.2c01668
ACS Sustainable Chem. Eng. 2022, 10, 8506−8516

Authors

Zhitong Zhao − *School of Materials Science and Engineering, Nanyang Technological University, Singapore 639798, Singapore;* orcid.org/0000-0003-1686-7074

Tao Xu − *Center for Nanotechnology and Nanotoxicology, Harvard T.H. Chan School of Public Health, Harvard University, Boston, Massachusetts 02115, United States;* orcid.org/0000-0002-1424-9363

Xiaoyong Pan − *School of Materials Science and Engineering, Nanyang Technological University, Singapore 639798, Singapore*

Susanti − *School of Biological Sciences, Nanyang Technological University, Singapore 639798, Singapore*

Jason C. White − *The Connecticut Agricultural Experiment Station, New Haven, Connecticut 06511, United States;* orcid.org/0000-0001-5001-8143

Xiao Hu − *School of Materials Science and Engineering, Nanyang Technological University, Singapore 639798, Singapore; Environmental Chemistry and Materials Centre, Nanyang Environment and Water Research Institute, Nanyang Technological University, 637141, Singapore;* orcid.org/0000-0002-0941-4205

Yansong Miao − *School of Biological Sciences, Nanyang Technological University, Singapore 639798, Singapore*

Philip Demokritou − *Center for Nanotechnology and Nanotoxicology, Harvard T.H. Chan School of Public Health, Harvard University, Boston, Massachusetts 02115, United States;* orcid.org/0000-0002-2484-9143

Complete contact information is available at: https://pubs.acs.org/10.1021/acssuschemeng.2c01668

Author Contributions

The article was written through contributions of all authors. All authors have given approval to the final version of the article. Specifically, Z.Z. planned and executed the experiments; T.X. helped to develop methodologies; X.P. fabricated and characterized the CD platform, S. planned and carried out the Arabidopsis experiments and analysis, J.C.W. helped to conceive the idea and formulated experimental strategies, X.H. conceived the CD platform and supervised relevant experiments, Y.M. supervised the Arabidopsis experiments and helped with data analysis, P.D. helped to conceive the idea, secured funding, developed methodologies, and analyzed the results, and K.W.N. conceived the idea, secured funding, developed the methodologies, and supervised the project team.

Notes

The authors declare no competing financial interest.

ACKNOWLEDGMENTS

The article was written through contributions of all authors. All authors have given approval to the final version of the article. This research is supported by Nanyang Technological University-Harvard T. H. Chan School of Public Health Initiative for Sustainable Nanotechnology (NTU-HSPH18004) the Ministry of Education, Singapore (AcRF Tier 1 RT10/20), and the National Research Foundation, Prime Minister's Office, Singapore, under its Campus for Research Excellence And Technological Enterprise (CREATE) and SHARE (Singapore HUJ Alliance for Research and Enterprise) program [REQ0246254 (NRF2020-THE003-0008)]. The authors acknowledge the Facility for Analysis, Characterization, Testing, and Simulation (FACTS), NTU, for the support in electron microscopy analysis.

REFERENCES

(1) Wielemaker, R.; Oenema, O.; Zeeman, G.; Weijma, J. Fertile Cities: Nutrient Management Practices in Urban Agriculture. *Sci. Total Environ.* **2019**, *668*, 1277−1288.

(2) Tomasi, N.; Pinton, R.; Dalla Costa, L.; Cortella, G.; Terzano, R.; Mimmo, T.; Scampicchio, M.; Cesco, S. New "solutions" for Floating Cultivation System of Ready-to-Eat Salad: A Review. *Trends Food Sci. Technol.* **2015**, *46*, 267−276.

(3) Asaduzzaman, M.; Kobayashi, Y.; Mondal, M. F.; Ban, T.; Matsubara, H.; Adachi, F.; Asao, T. Growing Carrots Hydroponically Using Perlite Substrates. *Sci. Hortic.* **2013**, *159*, 113−121.

(4) Goddek, S.; Joyce, A.; Kotzen, B.; Burnell, G. M. *Aquaponics Food Production Systems*; Springer: Cham, Switzerland, 2019. DOI: 10.1007/978-3-030-15943-6.

(5) Barbosa, G.; Gadelha, F.; Kublik, N.; Proctor, A.; Reichelm, L.; Weissinger, E.; Wohlleb, G.; Halden, R. Comparison of Land, Water, and Energy Requirements of Lettuce Grown Using Hydroponic vs. Conventional Agricultural Methods. *Int. J. Environ. Res. Public Health* **2015**, *12*, 6879−6891.

(6) Massa, D.; Magán, J. J.; Montesano, F. F.; Tzortzakis, N. Minimizing Water and Nutrient Losses from Soilless Cropping in Southern Europe. *Agric. Water Manag.* **2020**, *241*, 106395.

(7) Xiong, J.; Tian, Y.; Wang, J.; Liu, W.; Chen, Q. Comparison of Coconut Coir, Rockwool, and Peat Cultivations for Tomato Production: Nutrient Balance, Plant Growth and Fruit Quality. *Front. Plant Sci.* **2017**, *8*, 1−9.

(8) Chen, F.; Chai, H.; Song, Z.; Yu, L.; Fang, C. Hydrophilic Porous Polydimethysiloxane Sponge as a Novel 3d Matrix Mimicking Heterogeneous Pores in Soil for Plant Cultivation. *Polymers (Basel)* **2020**, *12*, 140.

(9) Verdoliva, S. G.; Gwyn-Jones, D.; Detheridge, A.; Robson, P. Controlled Comparisons between Soil and Hydroponic Systems Reveal Increased Water Use Efficiency and Higher Lycopene and β-Carotene Contents in Hydroponically Grown Tomatoes. *Sci. Hortic.* **2021**, *279*, 109896.

(10) Xu, T.; Ma, C.; Aytac, Z.; Hu, X.; Ng, K. W.; White, J. C.; Demokritou, P. Enhancing Agrichemical Delivery and Seedling Development with Biodegradable, Tunable, Biopolymer-Based Nanofiber Seed Coatings. *ACS Sustain. Chem. Eng.* **2020**, *8*, 9537−9548.

(11) Guo, H.; White, J. C.; Wang, Z.; Xing, B. Nano-Enabled Fertilizers to Control the Release and Use Efficiency of Nutrients. *Curr. Opin. Environ. Sci. Health* **2018**, *6*, 77−83.

(12) Wang, B.; Yang, W.; McKittrick, J.; Meyers, M. A. Keratin: Structure, Mechanical Properties, Occurrence in Biological Organisms, and Efforts at Bioinspiration. *Prog. Mater. Sci.* **2016**, *76*, 229−318.

(13) Ozaki, Y.; Takagi, Y.; Mori, H.; Hara, M. Porous Hydrogel of Wool Keratin Prepared by a Novel Method: An Extraction with Guanidine/2-Mercaptoethanol Solution Followed by a Dialysis. *Mater. Sci. Eng. C* **2014**, *42*, 146−154.

(14) Zhang, N.; Lai, H. Y.; Gautam, A.; De Kwek, D. Y.; Dong, Y.; Wang, Q.; Ng, K. W. An Enzymatic Method for Harvesting Functional Melanosomes after Keratin Extraction: Maximizing Resource Recovery from Human Hair. *J. Polym. Environ.* **2022**, *30*, 1045−1054.

(15) Hartrianti, P.; Nguyen, L. T. H.; Johanes, J.; Chou, S. M.; Zhu, P.; Tan, N. S.; Tang, M. B. Y.; Ng, K. W. Fabrication and Characterization of a Novel Crosslinked Human Keratin-Alginate Sponge. *J. Regen. Med. Tissue Eng.* **2017**, *11*, 2590−2602.

(16) Tan, B. Y.; Nguyen, L. T. H.; Kim, H.-S.; Kim, J.-H.; Ng, K. W. Cultivation of Human Dermal Fibroblasts and Epidermal Keratinocytes on Keratin-Coated Silica Bead Substrates. *J. Biomed. Mater. Res., Part A* **2017**, *105*, 2789−2798.

(17) Wang, S.; Wang, Z.; Foo, S. E. M.; Tan, N. S.; Yuan, Y.; Lin, W.; Zhang, Z.; Ng, K. W. Culturing Fibroblasts in 3D Human Hair Keratin Hydrogels. *ACS Appl. Mater. Interfaces* **2015**, *7*, 5187−5198.

(18) Wang, S.; Taraballi, F.; Tan, L. P.; Ng, K. W. Human Keratin Hydrogels Support Fibroblast Attachment and Proliferation in Vitro. *Cell Tissue Res.* **2012**, *347*, 795−802.
(19) Niculescu, M.-D.; Epure, D.-G.; Lasoń-Rydel, M.; Gaidau, C.; Gidea, M.; Enascuta, C. Biocomposites Based on Collagen and Keratin with Properties for Agriculture and Industrie Applications. *EuroBiotech J* **2019**, *3*, 160−166.
(20) Yoo, Y. K.; Kim, I. K.; Roh, M. S.; Roh, Y. S.; Huda, M. Growth, Flowering, and Nutrient Composition of Salvia Grown in Peat Moss Media Containing Pellets Processed with Poultry Feather Fibers at Different Mixing Ratios. *J. Hortic. Sci. Biotechnol.* **2017**, *35*, 289−299.
(21) Yin, X.-C.; Li, F.-Y.; He, Y.-F.; Wang, Y.; Wang, R.-M. Study on Effective Extraction of Chicken Feather Keratins and Their Films for Controlling Drug Release. *Biomater. Sci.* **2013**, *1*, 528−536.
(22) Yue, K.; Liu, Y.; Byambaa, B.; Singh, V.; Liu, W.; Li, X.; Sun, Y.; Zhang, Y. S.; Tamayol, A.; Zhang, P.; Ng, K. W.; Annabi, N.; Khademhosseini, A. Visible Light Crosslinkable Human Hair Keratin Hydrogels. *Bioeng. Transl. Med.* **2018**, *3*, 37−48.
(23) Ling, S.; Kaplan, D. L.; Buehler, M. J. Nanofibrils in Nature and Materials Engineering. *Nat. Rev. Mater.* **2018**, *3*, 1−15.
(24) Dinjaski, N.; Ebrahimi, D.; Qin, Z.; Giordano, J. E. M.; Ling, S.; Buehler, M. J.; Kaplan, D. L. Predicting Rates of in Vivo Degradation of Recombinant Spider Silk Proteins. *J. Regen. Med. Tissue Eng.* **2018**, *12*, e97−e105.
(25) Guan, Q.-F.; Han, Z.-M.; Zhu, Y.; Xu, W.-L.; Yang, H.-B.; Ling, Z.-C.; Yan, B.-B.; Yang, K.-P.; Yin, C.-H.; Wu, H.; Yu, S.-H. Bio-Inspired Lotus-Fiber-like Spiral Hydrogel Bacterial Cellulose Fibers. *Nano Lett.* **2021**, *21*, 952−958.
(26) Trache, D.; Tarchoun, A. F.; Derradji, M.; Hamidon, T. S.; Masruchin, N.; Brosse, N.; Hussin, M. H. Nanocellulose: From Fundamentals to Advanced Applications. *Front. Chem.* **2020**, *8*, 392.
(27) Deloid, G. M.; Sohal, I. S.; Lorente, L. R.; Molina, R. M.; Pyrgiotakis, G.; Stevanovic, A.; Zhang, R.; McClements, D. J.; Geitner, N. K.; Bousfield, D. W.; Ng, K. W.; Loo, S. C. J.; Bell, D. C.; Brain, J.; Demokritou, P. Reducing Intestinal Digestion and Absorption of Fat Using a Nature-Derived Biopolymer: Interference of Triglyceride Hydrolysis by Nanocellulose. *ACS Nano* **2018**, *12*, 6469−6479.
(28) Cheng, Y.-W.; Shiwarski, D. J.; Ball, R. L.; Whitehead, K. A.; Feinberg, A. W. Engineering Aligned Skeletal Muscle Tissue Using Decellularized Plant-Derived Scaffolds. *ACS Biomater. Sci. Eng.* **2020**, *6*, 3046−3054.
(29) Szymańska-Chargot, M.; Chylińska, M.; Gdula, K.; Kozioł, A.; Zdunek, A. Isolation and Characterization of Cellulose from Different Fruit and Vegetable Pomaces. *Polymers (Basel)* **2017**, *9*, 495.
(30) Deloid, G. M.; Cao, X.; Molina, R. M.; Silva, D. I.; Bhattacharya, K.; Ng, K. W.; Loo, S. C. J.; Brain, J. D.; Demokritou, P. Toxicological Effects of Ingested Nanocellulose in: In Vitro Intestinal Epithelium and in Vivo Rat Models. *Environ. Sci.: Nano* **2019**, *6*, 2105−2115.
(31) Khare, S.; DeLoid, G. M.; Molina, R. M.; Gokulan, K.; Couvillion, S. P.; Bloodsworth, K. J.; Eder, E. K.; Wong, A. R.; Hoyt, D. W.; Bramer, L. M.; Metz, T. O.; Thrall, B. D.; Brain, J. D.; Demokritou, P. Effects of Ingested Nanocellulose on Intestinal Microbiota and Homeostasis in Wistar Han Rats. *NanoImpact* **2020**, *18*, 100216.
(32) Bitounis, D.; Pyrgiotakis, G.; Bousfield, D.; Demokritou, P. Dispersion Preparation, Characterization, and Dosimetric Analysis of Cellulose Nano-Fibrils and Nano-Crystals: Implications for Cellular Toxicological Studies. *NanoImpact* **2019**, *15*, 100171.
(33) Lai, H. Y.; Wang, S.; Singh, V.; Nguyen, L. T. H.; Ng, K. W. Evaluating the Antioxidant Effects of Human Hair Protein Extracts. *J. Biomater. Sci., Polym. Ed.* **2018**, *29*, 1081−1093.
(34) Chua, H. M.; Zhao, Z.; Ng, K. W. Cryogelation of Human Hair Keratins. *Macromol. Rapid Commun.* **2020**, *41*, 2000254.
(35) Zhao, Z.; Moay, Z. K.; Lai, H. Y.; Goh, B. H. R.; Chua, H. M.; Setyawati, M. I.; Ng, K. W. Characterization of Anisotropic Human Hair Keratin Scaffolds Fabricated via Directed Ice Templating. *Macromol. Biosci.* **2021**, *21*, 2000314−9.
(36) Miao, C.; Hamad, W. Y. Cellulose Reinforced Polymer Composites and Nanocomposites: A Critical Review. *Cellulose* **2013**, *20*, 2221−2262.
(37) Xu, X.; Mao, X.; Zhuang, J.; Lei, B.; Li, Y.; Li, W.; Zhang, X.; Hu, C.; Fang, Y.; Liu, Y. PVA-Coated Fluorescent Carbon Dot Nanocapsules as an Optical Amplifier for Enhanced Photosynthesis of Lettuce. *ACS Sustain. Chem. Eng.* **2020**, *8*, 3938−3949.
(38) Yao, B.; Huang, H.; Liu, Y.; Kang, Z. Carbon Dots: A Small Conundrum. *Trends Chem.* **2019**, *1*, 235−246.
(39) Chung, S.; Revia, R. A.; Zhang, M. Graphene Quantum Dots and Their Applications in Bioimaging, Biosensing, and Therapy. *Adv. Mater.* **2019**, *33*, 1904362.
(40) Pietrini, F.; Carnevale, M.; Beni, C.; Zacchini, M.; Gallucci, F.; Santangelo, E. Effect of Different Copper Levels on Growth and Morpho-Physiological Parameters in Giant Reed (Arundo Donax L.) in Semi-Hydroponic Mesocosm Experiment. *Water (Switzerland)* **2019**, *11*, 1837−1856.
(41) Shen, Y.; Borgatta, J.; Ma, C.; Elmer, W.; Hamers, R. J.; White, J. C. Copper Nanomaterial Morphology and Composition Control Foliar Transfer through the Cuticle and Mediate Resistance to Root Fungal Disease in Tomato (Solanum Lycopersicum). *J. Agric. Food Chem.* **2020**, *68*, 11327−11338.
(42) Codling, E. E.; Schmidt, M. E.; Schmidt, W. F.; Huda, M. S. Keratin Nursery Pots as Potential Medium for Controlled Release of Copper Ions in Root Growth Control in Theobroma Cacao L. *J. Hortic.* **2019**, *6*, 2376−0354.
(43) Pyrgiotakis, G.; Luu, W.; Zhang, Z.; Vaze, N.; DeLoid, G.; Rubio, L.; Graham, W. A. C.; Bell, D. C.; Bousfield, D.; Demokritou, P. Development of High Throughput, High Precision Synthesis Platforms and Characterization Methodologies for Toxicological Studies of Nanocellulose. *Cellulose* **2018**, *25*, 2303−2319.
(44) Xu, K.; Wang, Z.; Copland, J. A.; Chakrabarti, R.; Florczyk, S. J. 3D Porous Chitosan-Chondroitin Sulfate Scaffolds Promote Epithelial to Mesenchymal Transition in Prostate Cancer Cells. *Biomaterials* **2020**, *254*, 120126.
(45) Keller, H.; Simak, P.; Schrepp, W.; Dembowski, J. Surface Chemistry of Thiols on Copper: An Efficient Way of Producing Multilayers. *Thin Solid Films* **1994**, *244*, 799−805.
(46) Tran, C. D.; Mututuvari, T. M. Cellulose, Chitosan and Keratin Composite Materials: Facile and Recyclable Synthesis, Conformation and Properties. *ACS Sustainable Chem. Eng.* **2016**, *4*, 1850−1861.
(47) Tran, C. D.; Mututuvari, T. M. Cellulose, Chitosan, and Keratin Composite Materials. Controlled Drug Release. *Langmuir* **2015**, *31*, 1516−1526.
(48) Kreitman, G. Y.; Danilewicz, J. C.; Jeffery, D. W.; Elias, R. J. Copper(II)-Mediated Hydrogen Sulfide and Thiol Oxidation to Disulfides and Organic Polysulfanes and Their Reductive Cleavage in Wine: Mechanistic Elucidation and Potential Applications. *J. Agric. Food Chem.* **2017**, *65*, 2564−2571.

https://doi.org/10.1021/acssuschemeng.2c01668
ACS Sustainable Chem. Eng. 2022, 10, 8506−8516